

Giant enhancement of the thermal Hall conductivity κ_{xy} in the superconductor $\text{YBa}_2\text{Cu}_3\text{O}_7$

Y. Zhang¹, N. P. Ong¹, P. W. Anderson¹, D. A. Bonn², R. Liang² and W. N. Hardy²

¹Joseph Henry Laboratories of Physics, Princeton University, Princeton, New Jersey 08544

²Department of Physics, University of British Columbia, Vancouver, Canada.

(May 9, 2019)

In high-purity crystals of $\text{YBa}_2\text{Cu}_3\text{O}_7$, the quasiparticle (qp) lifetime τ and the (weak-field) thermal Hall conductivity κ_{xy} undergo dramatic increases below 90 K. We present a detailed picture of the behavior of κ_{xy} at low temperature, in particular its scaling properties, which are directly relevant to the issue of whether Landau quantization of the qp states occurs.

The problem of excitations of the superconducting condensate in the cuprates at low temperatures is of strong current interest. In a d -wave superconductor, the energy-momentum dispersion of quasiparticles near a node is Dirac-like. The effect of an intense magnetic field on the quasiparticle (qp) states is an interesting open question [1–6]. Landau quantization of the qp states, first proposed by Schrieffer and Gorkov [1], has been recently re-derived using different arguments [2–4]. However, the case against Landau-level formation has also been argued [5,6].

A second problem is the temperature dependence of the qp mean-free-path ℓ (in zero field) close to T_c . Transport evidence from thermal conductivity [7], microwave and teraHertz experiments [8–10], and thermal Hall conductivity [13–15] point to a sharp increase in the qp lifetime just below T_c . Recent high-resolution angle-resolved photoemission (ARPES) experiments [11,12] have started to address the lifetime issue as well, but with conflicting results (see below).

These issues reflect the strong interest in the low-lying excitations of the d -wave superconductor. While microwave absorption and ARPES experiments provide valuable information on the quasiparticles, they are less effective in a field. For in-field experiments, teraHertz techniques [10] and the thermal Hall effect [13–15], in particular, have emerged as powerful probes of qp transport. In a field, the qp heat current develops a transverse component that is observed as a thermal Hall conductivity κ_{xy} (by contrast, phonons do not display a Hall effect since they are charge-neutral). Hence, κ_{xy} *selectively* senses the qp current alone [13]. To fully exploit this technique at low temperatures, however, samples with a very long ℓ are needed.

A recent innovation is the growth, using BaZrCO_3 (BZO) crucibles, of crystals of $\text{YBa}_2\text{Cu}_3\text{O}_y$ (YBCO) with nearly perfect crystalline order (from x-ray rocking curves [16]) and very low impurity concentration. The step-wise improvement in crystal quality results in strong enhancements of the qp lifetime τ . A number of novel features of qp heat transport become apparent in these crystals. The weak-field κ_{xy} undergoes a remark-

able thousand-fold increase between T_c and 30 K. Below 30 K, the curves of κ_{xy} vs H provide new, specific information on scaling behavior at low T [21]. Both features are directly relevant to the two issues mentioned above.

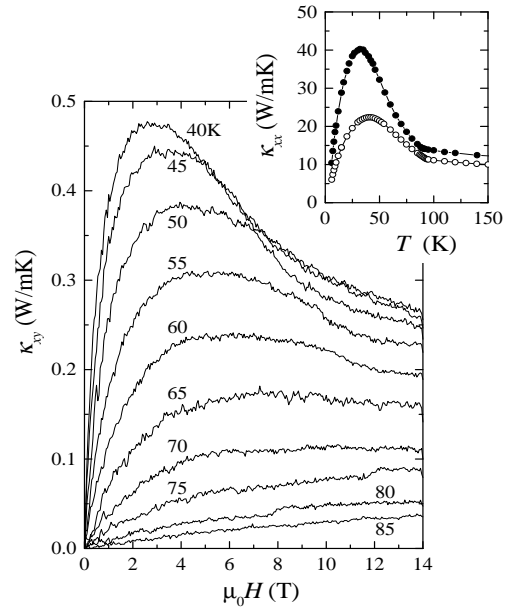


FIG. 1. (Main Panel) The thermal Hall conductivity κ_{xy} vs. H in BZO-grown $\text{YBa}_2\text{Cu}_3\text{O}_{6.99}$ ($T_c = 89$ K) at temperature from 85 to 40 K. As T decreases below T_c , the initial slope κ_{xy}^0/B increases sharply. The prominent peak in κ_{xy} below 55 K is a new feature in BZO-grown YBCO. The inset compares the zero-field $\kappa_{xx} \equiv \kappa_a$ in the BZO-grown crystal (solid circles) with a detwinned non-BZO grown crystal (open circles).

Among the cuprates, 90-K $\text{YBa}_2\text{Cu}_3\text{O}_7$ displays the largest in-plane thermal conductivity anomaly. In BZO-grown crystals, this anomaly is further enhanced, as shown in the inset in Fig. 1. The longitudinal thermal conductivity κ_{xx} ($-\nabla T \parallel \mathbf{a}$) in BZO crystals (solid circles) attains a peak value that is $\sim 80\%$ larger than that seen in typical, non-BZO detwinned crystals (open circles). To isolate the qp current, we turn to κ_{xy} . The main panel of Fig. 1 displays traces of κ_{xy} vs. field B from 85 to 40 K [17]. As in earlier studies [13,15], the ini-

tial slope $\kappa_{xy}^0/B \equiv \lim_{B \rightarrow 0} \kappa_{xy}/B$ increases very rapidly as the temperature T falls below T_c . Further, the curves are strongly non-linear in H . Both features reflect a τ that increases rapidly with decreasing T . An important new feature, absent in previous studies, is the prominent ‘overshoot’ that produces a maximum in κ_{xy} at the field scale H_{max} . As T falls below 40 K (see Fig. 2), the peak continues to narrow. For later reference, we note that, over a broad range of temperatures ($10 < T < 70$ K), H_{max} varies as T^2 . Moreover, at low temperatures ($T < 28$ K), the peak magnitude κ_{xy}^{max} also scales as T^2 .

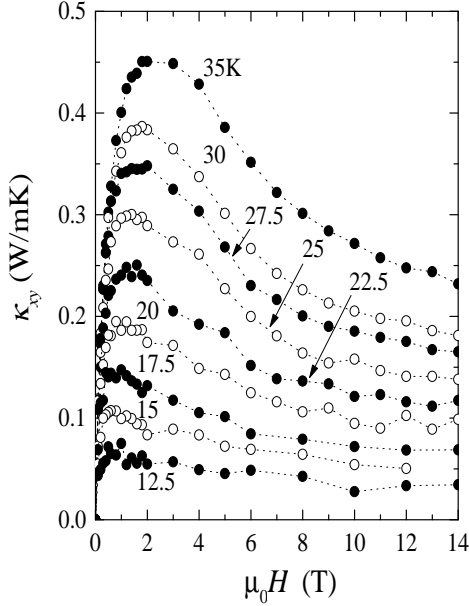


FIG. 2. The thermal Hall conductivity κ_{xy} vs. H in BZO-grown $\text{YBa}_2\text{Cu}_3\text{O}_{6.99}$ between 35 and 12.5 K. Below 28 K, the peak value varies as T^2 (see text).

The initial slope κ_{xy}^0/B , plotted as solid circles in Fig. 3, undergoes a thousand-fold increase between T_c and 30 K (the T -linear variation of κ_{xy} above T_c are displayed as open circles [18]). We now show that this giant enhancement is driven by a 100-fold increase in the qp lifetime.

To extract the zero-field mean-free-path (mfp) ℓ from κ_{xy}^0/B , we apply the Boltzmann-equation approach [19], which should be valid in the *weak*-field regime $\omega_c \tau \ll 1$ (ω_c is the cyclotron frequency). In terms of the ‘qp heat capacity’ $c_e = T^{-1} \sum_{\mathbf{k}} (-\partial f / \partial E_{\mathbf{k}}) E_{\mathbf{k}}^2$ where $E_{\mathbf{k}}$ is the qp energy, the zero- H thermal conductivity may be written as $\kappa_e = c_e (v\ell)/2$, with the group velocity $\mathbf{v}_{\mathbf{k}} = \nabla E_{\mathbf{k}}/\hbar$. (Close to a node \mathbf{k}^* , the qp energy may be approximated as $E_{\mathbf{q}} = \hbar \sqrt{(v_f q_1)^2 + (v_{\Delta} q_2)^2}$, where v_f and v_{Δ} are velocity parameters normal and parallel to the FS, and $\mathbf{q} = \mathbf{k} - \mathbf{k}^*$.)

The thermal Hall conductivity is related to κ_e by $\kappa_{xy} = \kappa_e \tan \theta$. We assume that, in the weak-field limit, the thermal Hall angle $\tan \theta$ is proportional to $\omega_c \tau$, viz.

$$\tan \theta = \eta \omega_c \tau = \eta \ell / k_F \ell_B^2, \quad (B \rightarrow 0) \quad (1)$$

where the magnetic length $\ell_B = \sqrt{\hbar/eB}$. The parameter η is less than 1 if ℓ is anisotropic around the FS. To obtain $\tan \theta$ [15], we first fit the profile of κ_{xx} vs. H to the empirical expression $\kappa_{xx}(B, T) = \kappa_e^0(T)/[1 + p|B|^{\mu}] + \kappa_{bg}(T)$, where the background term $\kappa_{bg}(T)$ is H -independent and identified with the phonon contribution. The initial Hall angle is then obtained as [15] $\tan \theta = \lim_{B \rightarrow 0} \kappa_{xy}(B)/[\kappa_{xx}(B) - \kappa_{bg}]$. This procedure allows us to extract $\tan \theta$ (hence, ℓ using Eq. 1).

As a consistency check, we adopt a second way to obtain ℓ from κ_{xy}^0 that relies on measurements of the electronic heat capacity c_e . Using Eq. 1, we may write

$$\kappa_{xy}^0 = \frac{c_e v_f \ell^2 \eta}{4 k_f \ell_B^2} \quad (2)$$

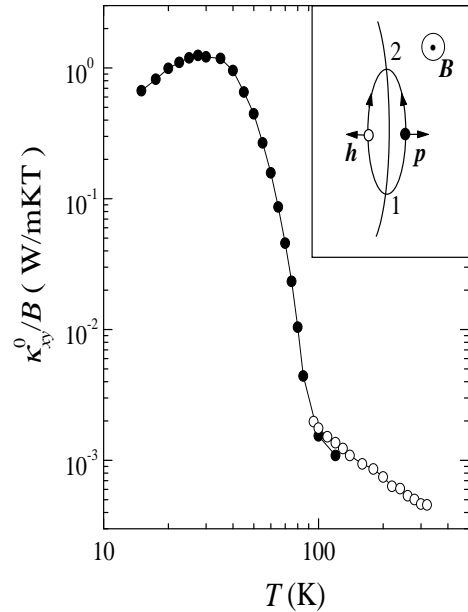


FIG. 3. The T dependence of the initial Hall slope κ_{xy}^0/B in BZO-grown YBCO (solid circles). Between T_c and 30 K, κ_{xy}^0/B increases by 10^3 . The $1/T$ dependence of κ_{xy}^0/B above T_c (measured in a non-BZO grown YBCO) is shown as open circles. The inset shows a qp energy contour on the Dirac cone. Group velocities on the particle- (p) and hole-like (h) branches are indicated.

In a d -wave superconductor, $c_e = \alpha_c T^2$ for $T < T_c$. Using the measured value $\alpha_c \simeq 0.064 \text{ mJK}^{-3} \text{ mol}^{-1}$ [20], we may invert Eq. 2 to find ℓ . We find that the values of ℓ obtained from the two methods share the *same* T dependence, but differ by a fixed factor of 1.5 if $\eta = 1$. By adjusting η to 0.6, we obtain numerical agreement between the two methods.

Figure 4 shows the T dependence of ℓ derived from the two methods. The agreement between the two sets of data is evidence that our assumption Eq. 1 is physically reasonable. Remarkably, between T_c and 20 K, the mfp increases by a factor of ~ 120 from 80 Å to 1 micron. In the expanded scale, we show that this increase is abrupt,

starting slightly below T_c .

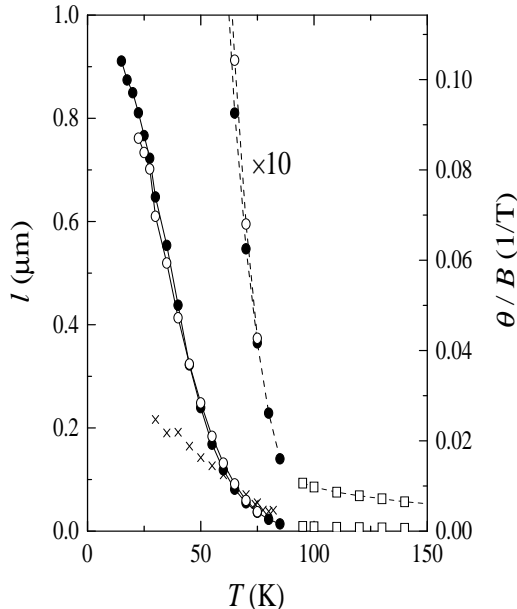


FIG. 4. The zero-field mean-free-path ℓ extracted from the weak-field Hall angle $\tan\theta$ (open circles), and from Eq. 2 (closed). The equivalent values of θ/B are shown on the right scale. The symbols (\times) represent $\tan\theta$ measured in a non-BZO detwinned YBCO crystal (Krishana *et al.* [14]). The expanded scale (dashed lines) highlights the steep increase below T_c . To extract ℓ , we used the values $\eta = 0.60$, $v_f = 1.78 \times 10^7$ cm/s, and $k_f = 0.8A^{-1}$.

[For comparison, $\tan\theta$ measured previously in a non-BZO crystal [15] is shown as \times . Based on the higher sensitivity and broader range in T in the present experiment, we now conclude that $\tan\theta$ does *not* lie on the extrapolated curve for the electrical Hall angle $\tan\theta_e$.]

Beyond the weak-field regime, we need a fully microscopic description of the qp thermal Hall current to properly analyze κ_{xy} vs. H . As the theoretical situation is unsettled, we adopt instead scaling arguments [21]. This approach reveals some rather striking features in the data.

For states close to the node \mathbf{k}^* , the linear energy dispersion $E = \hbar\bar{v}q$ (\bar{v} is an average velocity) implies a general relation between $k_B T$ and the magnetic length ℓ_B at a characteristic field scale B_s , viz.

$$k_B T = \hbar\bar{v}\sqrt{\frac{eB_s}{\hbar}}. \quad (3)$$

In addition to this general relation, Simon and Lee [21] have proposed that, at low T (< 30 K for YBCO), the magnitude of κ_{xy} should scale as

$$\kappa_{xy}(H, T) \sim T^2 F_{xy}(\sqrt{H}/\alpha T), \quad (4)$$

where $\alpha \equiv k_B/\bar{v}\sqrt{e\hbar}$, and $F_{xy}(u)$ is a scaling function of the dimensionless parameter $u = \sqrt{H}/\alpha T$. Hence, plots

of κ_{xy}/T^2 versus \sqrt{H}/T should collapse to the universal curve $F_{xy}(u)$.

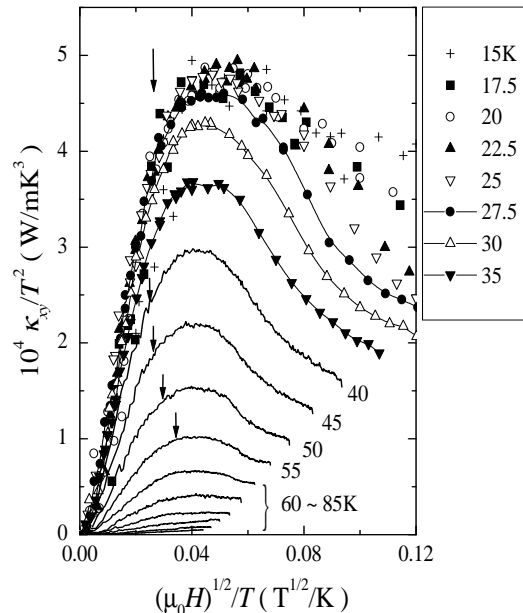


FIG. 5. Simon-Lee scaling plot of κ_{xy}/T^2 versus \sqrt{H}/T (Eq. 4). Below 28 K, the curves collapse onto a ‘universal’ curve $F_{xy}(u)$. Above 28 K, scaling is violated. However, the peaks still occur at the same x -coordinate ($\sqrt{H_{max}}/T = 0.042$). The arrows indicate the field scale H_{arc} .

We proceed to plot our results in this way in Fig. 5. While the curves above 28 K are spread out, the ones below collapse onto a common curve for $H < H_{max}$. The data taken at 25 K (and below) collectively determine the form of $F_{xy}(u)$. Its most notable feature is the nominally straight segment that extends from $u \simeq 0$ to just below $u_0 \equiv \sqrt{H_{max}}/\alpha T$, i.e. $F_{xy}(u) \sim u$ for $0 < u < u_0$. This simple form for F_{xy} implies that, below 25 K and for $H < H_{max}$, κ_{xy} reduces to the form

$$\kappa_{xy}(H, T) = C_0 T \sqrt{H}, \quad (5)$$

where the constant $C_0 = 1.51 \times 10^{-2}$ in SI units. Remarkably, when Eq. 5 applies, the magnitude of κ_{xy} is just proportional to $T\sqrt{H}$, and is insensitive to all transport quantities such as ℓ and θ . This interesting result has not been anticipated theoretically.

At larger values of u , F_{xy} attains a maximum value F_{xy}^0 before falling slowly. The T^2 dependence of the peak value κ_{xy}^{max} noted earlier in Fig. 2, is now seen to be a simple consequence of scaling behavior (i.e. $\kappa_{xy}^{max} \sim T^2 F_{xy}^0$).

Above 28 K, Simon-Lee scaling no longer holds. Three field regimes are now apparent. In weak fields ($0 < H < H_x$), κ_{xy} is strictly linear in H . Above H_x , we enter a regime reminiscent of the \sqrt{H} behavior at low- T (the H -linear regime is too small to resolve below 28 K). This

intermediate regime appears as straight-line segments in Fig. 5. Finally, closer to H_{max} , κ_{xy} deviates from \sqrt{H} behavior, and goes through a broad maximum. Surprisingly, as noted earlier, the weaker scaling relation in Eq. 3 continues to hold: Between 15 and 70 K, the maximum in κ_{xy} occurs at the *same* x -coordinate in Fig. 5, i.e. $\sqrt{H_{max}} = 0.042 T$. Substituting H_{max} for B_s in Eq. 3, we find that $\bar{v} \sim 8.0 \times 10^6$ cm/s, which is close to the geometric-mean velocity $\sqrt{v_f v_\Delta} \sim 6.8 \times 10^6$ cm/s (with $v_f = 1.78 \times 10^7$ cm/s [11] and $v_f/v_\Delta \sim 7$).

We may estimate semiclassically the time that an excitation, in a field, takes to move from 1 to 2 along the arc (inset, Fig. 3) by $\Delta t = (\hbar/eH) \int_1^2 ds_{\mathbf{k}} |\mathbf{v}_{\mathbf{k}}|^{-1}$, where $s_{\mathbf{k}}$ is the arc-length. For this time to equal τ , the field required is $H_{arc} = \pi E / (e v_\Delta v_f \tau)$. Using the measured $\ell \simeq v_f \tau$ at each T and setting $E = k_B T$, we indicate H_{arc} as arrows in Fig. 5. This rough estimate shows that the peak is related to the maximum arc length of the dominant energy contour on the Dirac cone. Hence, a detailed analysis of the Hall results should shed important light on the current debate about how vortices affect the qp spectrum. The presence of Landau Levels [1–4] or absence [5,6] will presumably have a large effect on κ_{xy} . Moreover, the direct measurement of the scaling function F_{xy} (Fig. 5) together with the other scaling features uncovered should stringently narrow the range of possibilities in this interesting problem.

The new results on κ_{xy} also bear on the issue of the change in qp lifetime at T_c . As discussed, ℓ derived from transport undergoes a steep increase just below T_c [7–9,13]. Recently, ARPES has attained enough resolution to probe the qp spectral peak along the nodal direction in $\text{Bi}_2\text{Sr}_2\text{CaCu}_2\text{O}_8$. Valla *et al.* [11] find that the width Δk ($\sim 1/\ell_{ARPES}$) retains its T -linear dependence across T_c (near T_c $\ell_{ARPES} \simeq 25 - 30 \text{ \AA}$). This appears to be in striking contrast with the transport results. However, Kaminski *et al.* [12] resolve a new feature of the qp peak that suggests a rather different picture. Below T_c , the qp width becomes dramatically narrower *provided it is probed within 60 mV of the Fermi energy*. They infer that well-defined qp states at the nodes exist only below T_c . The steep increase in ℓ shown in Fig. 4 is in close agreement with Kaminsky *et al.* The data in Fig. 4 show that ℓ increases to $\simeq 1 \mu\text{m}$ below 20 K (implying a peak 200 times narrower than the peaks resolved in the current ARPES studies). Hence, in high-purity YBCO, there are exceedingly sharp qp peaks in the spectral function that remain to be resolved and investigated. Understanding the abrupt appearance of the qp state below T_c , as implied by the steep increase in ℓ and κ_{xy}^0/B near T_c , seems a key problem in the cuprates.

The research is supported by the U.S. National Science Foundation (Grant NSF-DMR 9809483, at Princeton), and the Natural Science and Engineering Research Council (Canadian NSERC) and the Canadian Institute for Advanced research (CIAR) at U. British Columbia. N.P.O. also acknowledges support from the U.S. Office

of Naval Research (Contract N00014-98-10081) and the New Energy and Industrial Tech. Develop. Org., Japan (NEDO). We thank T.V. Ramakrishnan for valuable comments.

-
- [1] L. P. Gorkov and J. R. Schrieffer, Phys. Rev. Lett. **80**, 3360 (1998).
 - [2] P. W. Anderson, cond-mat/9812063.
 - [3] B. Jankó, Phys. Rev. Lett. **82**, 4703 (1999).
 - [4] N. B. Kopnin and V. M. Vinokur, preprint 2000.
 - [5] A. S. Mel'nikov, J. Phys.: Condens. Matter, **11**, 4219 (1999).
 - [6] M. Franz and Z. Tesanovic, cond-mat/9903152.
 - [7] R.C. Yu, M. B. Salamon, J. P. Lu, and W. C. Lee, Phys. Rev. Lett. **69**, 1431 (1992).
 - [8] D. A. Bonn *et al.*, Phys. Rev. Lett. **68**, 2390 (1992); A. Hosseini *et al.*, Phys. Rev. B **60**, 1349 (1999).
 - [9] Martin C. Nuss *et al.*, Phys. Rev. Lett. **66**, 3305 (1991).
 - [10] S. Spielman, Beth Parks, J. Orenstein *et al.*, Phys. Rev. Lett. **73**, 1537 (1994); B. Parks *et al.*, *ibid.*, **74**, 3265 (1995).
 - [11] T. Valla *et al.*, Science **285**, 2110 (1999).
 - [12] A. Kaminski *et al.*, Phys. Rev. Lett. **84**, 1788 (2000).
 - [13] K. Krishana, J. M. Harris, and N. P. Ong, Phys. Rev. Lett. **75**, 3529 (1995).
 - [14] B. Zeini *et al.*, Phys. Rev. Lett. **82**, 2175 (1999).
 - [15] K. Krishana *et al.*, Phys. Rev. Lett. **82**, 5108 (1999).
 - [16] Ruixing Liang, D.A. Bonn and W.N. Hardy, Physica C **304**, 105 (1998).
 - [17] With the thermal gradient $-\nabla T \parallel \mathbf{a} \parallel \mathbf{x}$ and the field $\mathbf{H} \parallel \mathbf{c} \parallel \mathbf{z}$, the thermal Hall current is $\parallel \mathbf{y}$. Above 35 K, the 'Hall' gradient $-\partial_y T$ is measured continuously with a chromel-constantan thermocouple as H is swept slowly (0.2 T/min.). Below 35 K (Fig. 2), we adopt a high-resolution mode. Each point is taken with H stabilized. The signal is sampled with $-\partial_x T$ turned on, then off. Each Hall trace is the average of two traces, from -14 to 14 T and from 14 to -14 T.
 - [18] Y. Zhang *et al.*, Phys. Rev. Lett. **84**, 2219 (2000).
 - [19] J. Bardeen, Rickayzen, Tewordt, Phys. Rev. **113**, 982 (1959).
 - [20] D. A. Wright *et al.*, Phys. Rev. Lett. **82**, 1550 (1999).
 - [21] Steve H. Simon and Patrick A. Lee, Phys. Rev. Lett. **78**, 1548 (1997).